ADVANCED MATERIALS INTERFACES
www.advmatinterfaces.de

Thermal and pH Sensitive Composite Membrane for On-Demand Drug Delivery by Applying an Alternating Magnetic Field

*Ya Wang, Giovanni Boero, Xiaosheng Zhang, and Juergen Brugger**

Implantable drug delivery systems that can realize a scheduled drug release according to the needs of patients would be highly beneficial for the treatment of chronic diseases and cancer. Here, micrometer-sized hydrogel particles with both thermal and pH sensitivities are fabricated for the first time and embedded with magnetic nanoparticles in silk fibroin to generate a composite membrane. The permeability of the membrane is adjustable reversibly by temperature and pH. Promptly responded drug release within 1 min by applying an alternating magnetic field is demonstrated with the membrane. The on/off switching of an alternating magnetic field (16 mT, 111 kHz) induces heat generation by the magnetic nanoparticles resulting in a reversible change of the membrane permeability due to the shrinking/swelling of the microgels. A control over two orders of magnitude of the release rate (0.01–5.0 µg min^{-1}) of Rhodamine B (Rh.B) model drug is achieved by tuning the content of microgels and magnetic nanoparticles, as well as the thickness of the membrane. Additionally, an increase in the release rate of Rh.B in acidic condition with respect to the physiological pH value is demonstrated. This represents an additional functionality of the implantable membrane with relevant features for spatially selective cancer treatment.

Even though controlled drug delivery systems have been intensively investigated in the past few decades, most of the previous works focus on sustaining the drug concentration within the therapeutic window for an extended period after a one-time trigger.[1–3] Regardless of patients' needs and varying physiological environments, such a monotonic release method with no flexibility of adjusting release timing and dosage is not optimal for certain diseases such as diabetes, chronic pain, and cancer.[4–6] Thus, on-demand drug delivery systems that allow multiple dosing by repeated triggering are highly needed.

A magnetic field is well suited as an external trigger for these applications because it is harmless and allows for spatio-temporal control. Upon stimulation by an alternating magnetic field, magnetic nanoparticles are capable of converting electromagnetic energy into heat via Brownian and Néel relaxation.[7] In previous works, the control of the drug release was performed by the physical deformation of a magnetic membrane/sponge under an external static magnetic field produced by a permanent magnet.[4,8] This actuation method requires an accurate alignment between the magnet and the membrane/sponge. Another work reported the fabrication of an ethylcellulose membrane with thermosensitive nanogels and magnetic nanoparticles. Based on the reversible shrinkage of the nanogels as a result of magnetic heating, the permeability of the membrane was changed accordingly to release the drug repeatedly. However, the onset of drug release could take up to 50 min after turning on the magnetic field and no control of the release rate (0.01 mg min^{-1}) was demonstrated.[9] A follow-up work succeeded to control the release rate thermally by changing the environmental temperature, although when the system was activated by the magnetic field, release rate only at the same order (4.1 and 5.7 µg min^{-1}) was shown and a 10–30 min time lag was observed for the release.[10]

Thermal sensitive hydrogel particles with crosslinked poly(N-isopropylacrylamide) (PNIPAM) have been intensively studied over the last decade for drug delivery application.[11–14] They undergo sharp and reversible volume phase transition at the lower critical solution temperature due to the balance between hydrophilic and hydrophobic forces.[15] So far, the majority of the obtained PNIPAM hydrogel particles were limited in the range of hundreds of nanometers, only a few were reported to have micrometer sizes.[16–18] Since micrometer-sized PNIPAM particles have a higher swelling capacity compared with the conventional nanometer-sized ones, a larger volume shrinkage can be generated under the same condition, and faster drug release can be expected. All previously published micrometer-sized PNIPAM particles have a phase transition temperature

Y. Wang, Dr. G. Boero, Prof. J. Brugger
Microsystems Laboratory
École Polytechnique Fédérale de Lausanne
Lausanne 1015, Switzerland
E-mail: juergen.brugger@epfl.ch
Prof. X. S. Zhang
School of Electronic Science and Engineering
University of Electronic Science and Technology of China
Chengdu 611731, China
The ORCID identification number(s) for the author(s) of this article can be found under https://doi.org/10.1002/admi.202000733.

© 2020 The Authors. Published by WILEY-VCH Verlag GmbH & Co. KGaA, Weinheim. This is an open access article under the terms of the Creative Commons Attribution License, which permits use, distribution and reproduction in any medium, provided the original work is properly cited.

DOI: 10.1002/admi.202000733

of around 32 °C. Since they are fully collapsed at the physiological temperature of 37 °C, the drug release would be always "on" and, when implanted in the human body, no control over time would be possible. Ideally, for drug delivery applications, micrometer-sized PNIPAM particles should have a phase transition temperature slightly higher than 37 °C.

Besides thermal sensitivity, pH sensitivity is also very beneficial. The extracellular environment of a tumor has an acidic pH (5–7) due to the high rate of glycolysis in cancer cells.[19–20] pH sensitive drug delivery systems have been developed for selective cancer treatment based on the physiological differences between tumors and healthy tissues.[21–23] The ideal pH sensitive drug delivery system for cancer therapy should have fast drug release at the acidic condition and slow or no release at the physiological condition. PNIPAM particles can be engineered to have the desired pH sensitivity by copolymerization with an acidic monomer. When the pH sensitive PNIPAM particles are exposed to an environment with pH larger than pKa, which is around 5 for methacrylic acid, electrostatic repulsion restricts the shrinkage of the microgel and therefore prevents drug release.

Here we report a fast responsive, on-demand drug delivery system that can be repeatedly switched on and off via an alternating magnetic field. A composite membrane is prepared from silk fibroin (supporting membrane), thermal/pH sensitive PNIPAM-based microgels (responding agents), and magnetic nanoparticles (local heating sources). When the membrane is exposed to an alternating magnetic field (in our case of about 16 mT at 111 kHz), the magnetic nanoparticles generate heat, inducing the shrinkage of the microgels and the release of Rhodamine B (model drug), as illustrated in **Figure 1**. When the magnetic field is off, without the heating from magnetic nanoparticles, the microgels swell back to their original size and the release of Rh.B is impeded. Additionally, since the microgel has a lower volume phase transition temperature (VPTT) at acid pH than at physiological one, a much higher release rate of Rh.B is observed in the former case than the latter one, a feature that can be exploited for spatially selective cancer therapy.

The N-isopropylacrylamide (NIPAM)-based hydrogel particles in micrometer scale size are synthesized by precipitation polymerization with three monomers: N-isopropylacrylamide (NIPAM), N-isopropylmethacrylamide (NIPMAM) and methacrylic acid (MAA). The morphology of the microgel at the dried state is observed by scanning electron microscope (Figure 1d). The microgels are spheres with core-shell structures and have a diameter of around 1 μm. The same structures are imaged by atomic force microscope and the height profile indicates that the core diameter is around 760 nm and the shell thickness is around 170 nm (Figure S1, Supporting Information).

To investigate the thermal responsiveness of the microgel, dynamic light scattering (DLS) is used to measure its diameter at different temperatures. As expected and shown in **Figure 2**a, the size of the microgel is in inverse correlation with the temperature. For instance, the size of the microgel at pH 5.0 decreases from 2.1 to 0.75 μm when the temperature increases from 25 to 60 °C, and the volume phase transition temperature (VPTT) is found to be around 38 °C. More importantly, due to the presence of methacrylic acid (pKa 5) (see FTIR measurement in Figure S2a, Supporting Information), the obtained microgel is expected to behave differently at different pH values. When pH increases from 5.0 to 7.4, the size of the microgel measured at the same temperature increases, and a higher temperature is required to initiate the shrinkage of the microgel. As summarized in Figure 2b, when pH increases from 5.0 to 7.4, the VPTT increases from 38 to 44 °C, while the diameter shrinkage decreases from 65% to 48%, and the corresponding volume shrinkage decreases from 96% to 86%. The explanation for this phenomenon is as follows. When the pH is higher than the pKa of methacrylic acid, the deprotonation reaction is undergoing, which increases the electrostatic repulsion of the microgel and leads to a larger extent of swelling shown as the larger size. Meanwhile, it also limits the shrinkage of microgel when the temperature increases, which requires a higher temperature to start shrinking and decreases the shrinkage size and volume accordingly.

Iron oxide nanoparticles with saturation magnetization of around 44 emu g^{-1} and superparamagnetic behavior are prepared in the first step (Figure S3, Supporting Information). Then composite silk fibroin membranes (10–40 μm) with microgels (MGs) and synthesized magnetic nanoparticles (MNPs) are fabricated by the solution casting method with a mixed solution of the three components. The as-prepared membranes are treated with ethanol (EtOH) to make them water-stable by inducing β-sheet structures inside (Figure S4, Supporting Information). By changing the components' ratio, membranes with varying content of microgels (17, 29, and 45 wt%) and MNPs (9, 13, and 17 wt%) are fabricated (**Table 1** and Figure S5, Supporting Information).

To demonstrate the potential of utilizing the prepared composite membranes for controllable drug delivery by tuning the size of loaded microgels via temperature or pH, a fluorescence dye Rhodamine B (Rh.B) is used as a model drug to test its release profiles. The identical membrane E is tested at varying temperatures from 25 to 55 °C in both acetate buffer (pH 5.0) and phosphate-buffered saline (PBS, pH 7.4). As shown in Figure 2c, at pH 5.0, the released amount of Rh.B in 24 h increases with temperature until 45 °C. From 45 to 55 °C, the released amount is almost temperature independent. This correlates well with the microgel size tested at pH 5.0, which decreases significantly from 25 to 45 °C, and is almost constant from 50 to 55 °C. However, the Rh.B release at pH 7.4 is found to be very slow in the range of 25–40 °C and then increases above 40 °C due to the fact that the onset temperature of microgel shrinkage is about 40 °C at pH 7.4. As expected, Rh.B is released much faster at pH 5.0 than pH 7.4 when tested at the same temperature, which is due to the relatively smaller microgel size in the former case. Hence, it is demonstrated here that a precisely controlled Rh.B release can be achieved with the composite membrane by changing its permeability due to the phase change of loaded microgels via temperature and pH. The Rh.B release at pH 5.0 starts at a lower temperature with a higher release rate than that at pH 7.4.

After demonstrating that the prepared membrane can be used for controlled Rh.B release by changing the temperature and pH, we investigate how the content of microgels (MGs) and the membrane thickness influence the release kinetics. The released Rh.B amount increases almost linearly with time (Figure S7, Supporting Information), and the color of the reservoir is unchanged even after 24 h indicating no release of Rh.B through the 3D printed reservoir. In order to understand better how fast the Rh.B release is for each membrane tested at

© 2020 The Authors. Published by WILEY-VCH Verlag GmbH & Co. KGaA, Weinheim

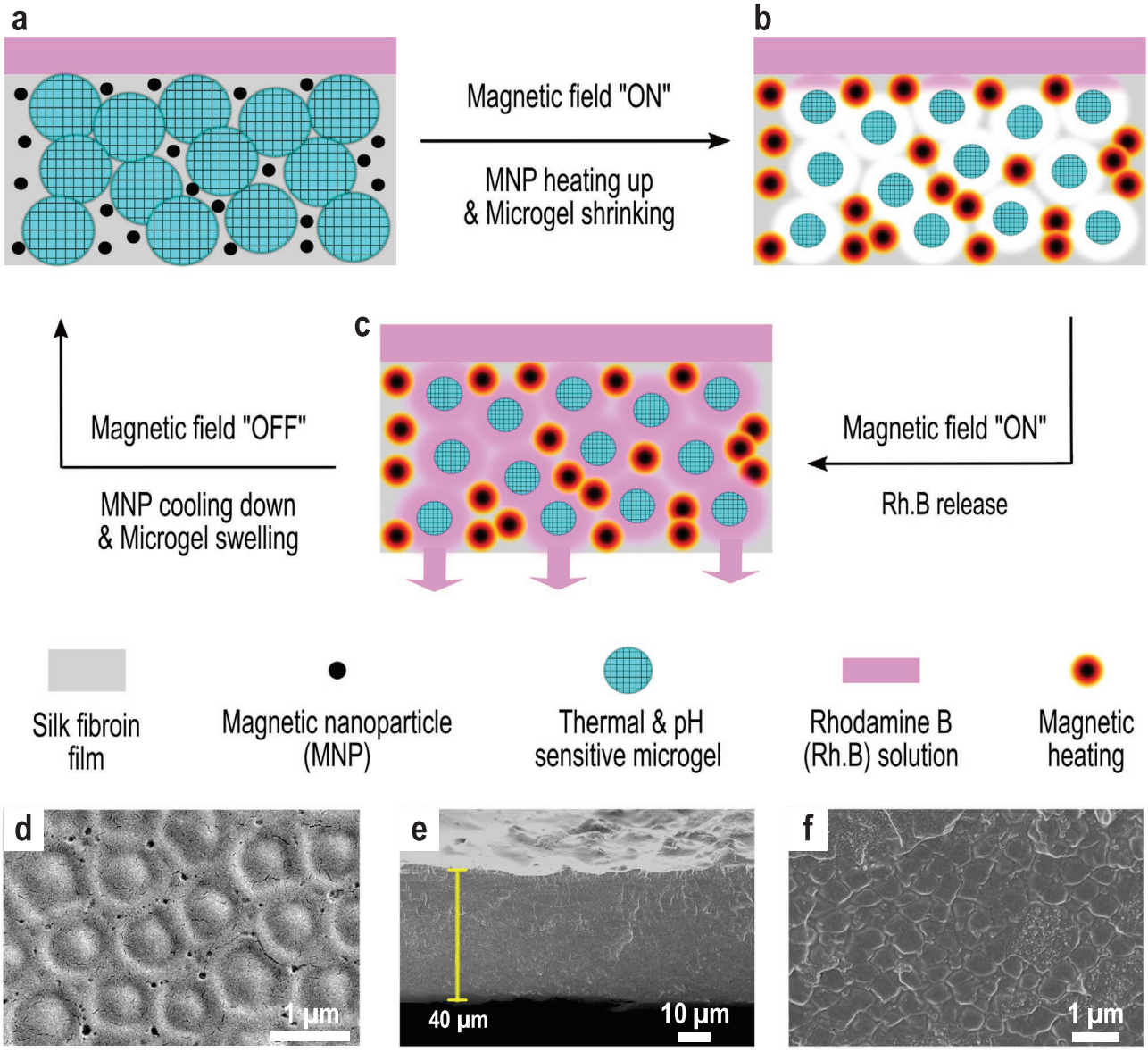

Figure 1. Silk composite membrane with magnetic nanoparticles and thermal/pH sensitive microgels for drug delivery controlled by an external magnetic field. Rhodamine B (Rh.B) fluorescence dye is used as a model drug to demonstrate the working principle. a) When the composite membrane is exposed to an alternating magnetic field, b) the magnetic nanoparticles are locally heated up, and lead to the shrinkage of microgels and generate free volume inside the membrane, c) through which Rh.B can be released quickly. When the magnetic field is turned off, the magnetic nanoparticles cool down, the microgels swell back to their original size, and the release of Rh.B is impeded. The red shell around the magnetic nanoparticles illustrates the increase of temperature in the region in close proximity to the nanoparticle due the presence of the alternating magnetic field. Since the microgels are more sensitive to temperature changes at the acidic condition than at the physiological one, much higher Rh.B release rate is obtained when the surrounding environment is acidic, such as in a tumor area. Therefore, on-demand Rh.B can be achieved due to the reversible shrinking/swelling behavior of microgel via stimulation by the magnetic field. d) Scanning electron microscope images of e) microgels in the dried state and f) cross-sectional surfaces of the composite membrane.

different conditions, linear fitting is applied to the above curves, and the release rate (the slop) is plotted against the weight percentage of microgels (**Figure 3**).

Firstly, for the identical membrane tested at different temperatures and pH, the higher the temperature and the more acidic the pH, the faster is the release rate. Taking membrane A as an example (Figure 3a), the Rh.B release rate is 269 μg h^{-1} (pH 5.0 at 45 °C), 153 μg h^{-1} (pH 5.0 at 25 °C), 43 μg h^{-1} (pH 7.4 at 45 °C), and 1.9 μg h^{-1} (pH 7.4 at 25 °C) respectively. Therefore, a control over two orders of magnitude (1.9–269 μg h^{-1}) of Rh.B flux can be obtained by changing the environmental temperature and pH. Secondly, by adjusting the loading content of microgels embedded inside the membrane, the release rate can be tuned accordingly. With a higher loading amount, the permeability of the membrane changes more significantly due to microgel shrinkage, which results in

© 2020 The Authors. Published by WILEY-VCH Verlag GmbH & Co. KGaA, Weinheim

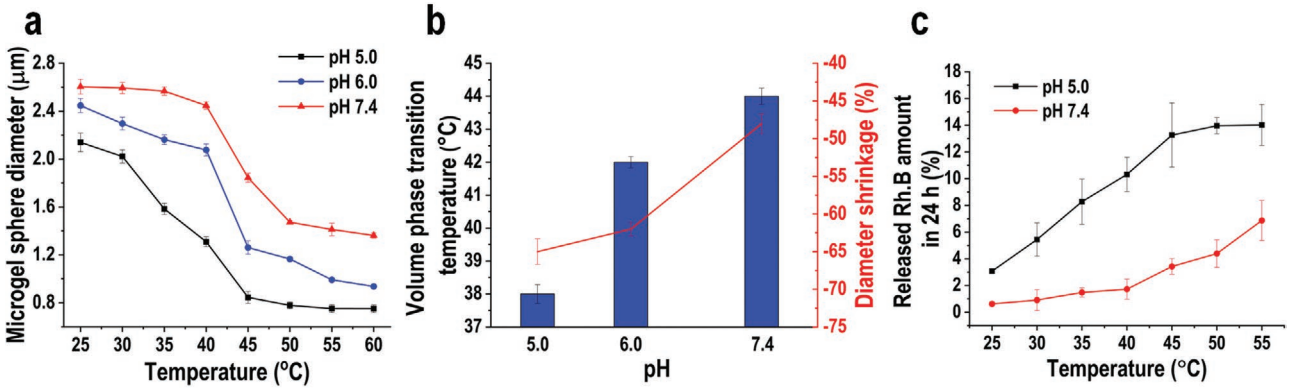

Figure 2. a) Investigation of the effect of pH and temperature on the microgel diameter. The diameter of microgel sphere at pH 5.0, 6.0, and 7.4 in the temperature range from 25 to 60 °C is measured by dynamic light scattering (DLS). The error bars indicate the standard deviation computed from three independent measurements. b) Influence of pH on the volume phase transition temperature (VPTT) and the related diameter change after fully shrinking of microgels. c) Study of the relationship of Rh.B release amount versus the temperature in acetate buffer (pH 5.0) and phosphate-buffered saline (PBS, pH 7.4) with membrane E (Silk/MGs/MNPs = 59/29/12, 15 μm). The tested period is 24 h. The error bars indicate the standard deviation computed from the measurements on three nominally identical membranes.

a faster release rate. For membrane E which has only 29 wt% MGs, the release rate of Rh.B is less than that of membrane A (45 wt% MGs), which is reduced to 114 μg h^{-1} (pH 5.0 at 45 °C), 32 μg h^{-1} (pH 5.0 at 25 °C), 18 μg h^{-1} (pH 7.4 at 45 °C), and 1.7 μg h^{-1} (pH 7.4 at 25 °C). For membrane G which has the least content of microgels (17 wt%), even the largest achieved release rate (pH 5.0 at 45 °C) is rather slow (11 μg h^{-1}). Therefore, in order to achieve a relatively high release rate, at least 29 wt% of microgels are required. Lastly, since Rh.B release from the membrane is mainly a diffusion-driven process, adjusting the thickness is another straightforward method to tune the release rate. With increased path length for Rh.B molecules to pass through the membrane by increasing the thickness, the release is expected to be slowed down. Membranes (B, F, and H) with larger thickness are also tested in the same condition. As shown in Figure 3b, when the membrane thickness is increased to 30–40 μm, the release rate decreases significantly. For example, the Rh.B release rate for membrane B (45 wt% MGs) is reduced to 58 μg h^{-1} (pH 5.0 at 45 °C), 16 μg h^{-1} (pH 5.0 at 25 °C), 13 μg h^{-1} (pH 7.4 at 45 °C), and 0.5 μg h^{-1} (pH 7.4 at 25 °C) respectively. Larger release flux through thin membranes compared to the flux through thick membranes can be observed clearly from the images in Figure S8 (Supporting Information). If the content of microgels is reduced to 29 wt% (membrane F), the release rate is rather slow (10 μg h^{-1}) even when it is tested in pH 5.0 at 45 °C. For membrane H (17 wt% MGs), the release rates are further reduced to less than 1 μg h^{-1}.

Table 1. Details of the prepared membranes, having different mass ratios between silk fibroin, microgels (MGs), and magnetic nanoparticles (MNPs), and thicknesses (as measured by SEM).

Parameter	Membrane	Thickness [μm]	Silk fibroin weight [mg]	MGs weight [mg]	MNPs weight [mg]	Silk fibroin weight percentage [wt%]	MGs weight percentage [wt%]	MNPs weight percentage [wt%]
Membrane thickness	A	20	45	45	9	45	45	9
	B	40	90	90	18	45	45	9
	E	15	45	22.5	9	59	29	12
	F	40	90	45	18	59	29	12
	G	10	45	11.25	9	69	17	14
	H	30	90	22.5	18	69	17	14
Content of magnetic nanoparticles (MNPs)	A	20	45	45	9	45	45	9
	C	20	45	45	13.5	43	43	13
	D	25	45	45	18	42	42	17
Content of microgels (MGs)	A	20	45	45	9	45	45	9
	E	15	45	22.5	9	59	29	12
	G	10	45	11.25	9	69	17	14
	B	40	90	90	18	45	45	9
	F	40	90	45	18	59	29	12
	H	30	90	22.5	18	69	17	14

© 2020 The Authors. Published by WILEY-VCH Verlag GmbH & Co. KGaA, Weinheim

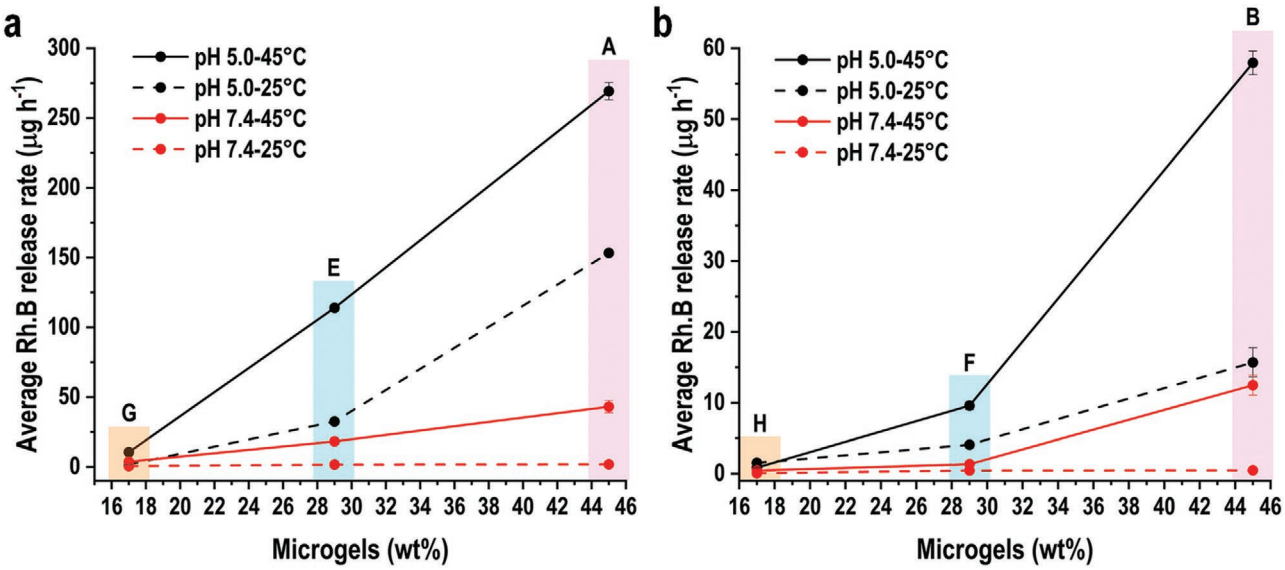

Figure 3. Thermally and pH triggered Rh.B release with Silk/MGs/MNPs composite membranes. The Rh.B release rate for a) thin membranes (10–20 μm) (A, E, and G) and b) thick membranes (30–40 μm) (B, F, and H) measured in both acetate buffer (pH 5.0) and phosphate-buffered saline (PBS, pH 7.4) at 45 °C and at 25 °C. The error bars indicate the standard deviation computed from the measurements on three nominally identical membranes.

Since magnetic nanoparticles are capable of transforming the electromagnetic energy to heat when exposed to an alternating magnetic field, the final goal is to use magnetic nanoparticles as local heating sources to induce shrinking of microgels and facilitate Rh.B release through the membrane. Firstly, the effect of MGs' loading content on the release behavior is investigated with membrane A, C, and D. Similar release profiles are observed (Figure S10, Supporting Information), where we can see that with more magnetic nanoparticles inside the membrane, higher heating efficiency is achieved. Thus, it results in a higher average temperature gradient ΔT (Table S1, Supporting Information), which contributes to a faster release of Rh.B.

After turning on the magnetic field, the release starts within 1 min detected by naked eyes and the first sample is collected and tested by UV–vis after 5 min (**Figure 4**a). At pH 5.0, the released Rh.B amount after three successive on (2 h) /off (2 h) cycles of the magnetic field is 1.9% for membrane A, 7.5% for membrane C, and 20% for membrane D. Hence, for membranes with the same content of MGs and similar thickness, a larger content of MNPs generates more heating which ultimately leads to a higher release rate of Rh.B.

Secondly, since the release of Rh.B through the membrane is due to diffusion, membranes with a larger thickness (i.e., longer diffusion path) are tested to study its effect on the Rh.B release. For membrane B, having the same contents of MGs and MNPs but the double thickness with respect to membrane A, the released content increases to 3.6%, even though the release of Rh.B starts after 15 min when the magnetic field is firstly turned on. When the membrane's thickness increases, the released content increases. This is because the absolute mass of MNPs is higher for a thicker membrane even though the ratio is kept the same. This is the opposite of the previous results where the Rh.B release is triggered by changing homogenously the environment temperature or pH (Figure 3). Since the heating efficiency is proportional to the amount of magnetic nanoparticles in the membrane, thicker membranes would allow to achieve a faster release rate in presence of the magnetic field excitation.

Thirdly, as thermal responsive agents, the content of MGs influences the release behavior significantly. If the content of MGs is reduced, for the thin membrane E, the release starts still within 1 min after turning on the magnetic field, but the released Rh.B amount is only 0.13% after three successive on/off cycles of the magnetic field. When the thickness is doubled, for membrane F, the release of Rh.B starts after 440 min regardless of whether the magnetic field is on or off, the release rate is slow and the released amount is only 0.02%. Based on what has been found above, for silk fibroin membranes with 9 wt% MNPs, larger than 29 wt% MGs are needed in order to achieve an effectively high release rate of Rh.B with the magnetic field as the stimulus. For membranes with unsufficient microgels inside to form connected channels, the release rate is primarily dependent on the membrane thickness, the larger thickness slows down the release rate. By tuning the content of MGs and MNPs, and the thickness of the membrane, a control over two orders of magnitude of the release rate (0.01–5.0 μg min^{-1}) is achieved (Figure 4c).

Lastly, when the identical membranes are tested in PBS buffer, the released amount of Rh.B is significantly reduced and no more than 0.8% is released after the same period of time (Figure 4b). For thin membranes A, C, D (20–25 μm) with similar contents of MGs, the Rh.B release starts also within 1 min after the magnetic field is switched on. Overall, the release rate is slower than that in acetate buffer, and no significant differences are observed even when the content of MNPs is increased to 17 wt%. This is due to the fact that a higher temperature is needed to initiate MGs shrinkage at pH 7.4. For the thicker membrane B with 45 wt% MGs, the release starts 75 min after

© 2020 The Authors. Published by WILEY-VCH Verlag GmbH & Co. KGaA, Weinheim

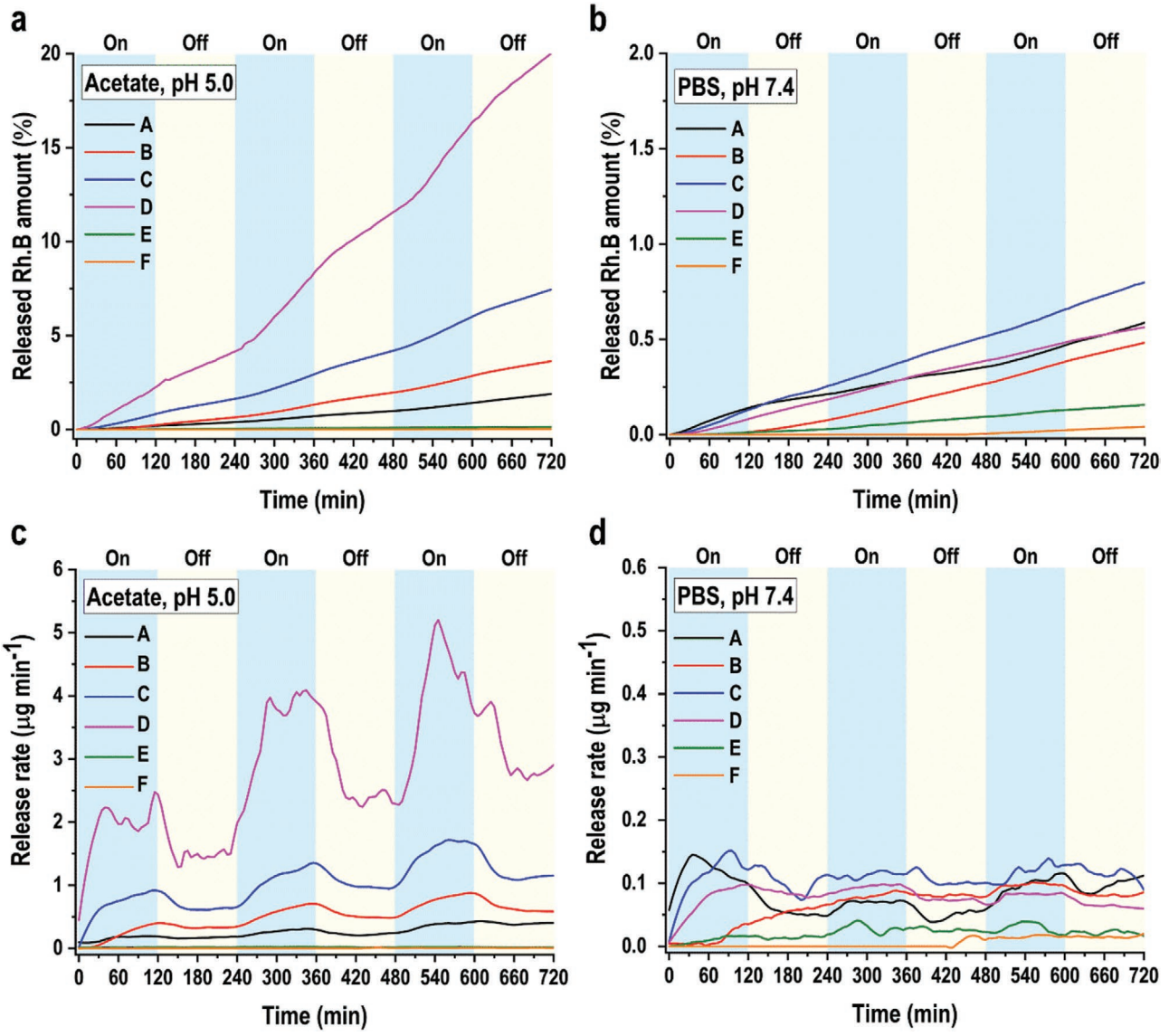

Figure 4. Rh.B release triggered by an alternating magnetic field of 16 mT at 111 kHz. The released Rh.B amount (%) is measured in a) acetate buffer (pH 5.0) and b) PBS (pH 7.4). From these measurements, the release rates are computed and shown in c) acetate buffer (pH 5.0) and d) PBS (pH 7.4). Note that the scales on the ordinates of the graphs (a,c) are ten times larger than those on graphs (b,d).

switching on the magnetic field (Figure S11, Supporting Information), and the release rate increases until saturation even when the magnetic field is switched off (Figure 4d). There is a small increase when the magnetic field is on due to the temperature increase and then drops back to the saturation level when it is off. For membranes E and F, the release profiles are almost the same as those in acetate buffer. For membrane F, the release of Rh.B also starts after 440 min no matter if the state of the magnetic field is on or off. According to the SEM images shown in Figure S12 (Supporting Information), a 29 wt% MGs content is not sufficient to form connected channels, and thus Rh.B is released at a slow rate. As shown in Figure 4d, the release rates for membranes A, B, C, D are much smaller than that in acetate buffer, which are below 0.15 μg min^{-1}. For membranes E and F, it is almost the same as that in acetate buffer, with a release rate smaller than 0.05 μg min^{-1}.

In addition, we also prepare control materials including silk fibroin/magnetic nanoparticles (silk/MNPs) membrane and silk fibroin/microgels (silk/MGs) membrane to investigate the differences in Rh.B release behavior. The release of Rh.B through silk/MNPs membrane is very slow at the beginning and then almost linear release begins after 6 days (Figure S13, Supporting Information). This type of membrane does not allow the control of the release time and amount. For silk/MGs membrane with only microgels, the membrane is too fragile mechanically to be used to seal the reservoir for release applications.

We present a responsive membrane for adjusting the release rate of a drug substance that can be controlled by two functionalities: thermal and pH. The effect is reversible and is based on a new thermal and pH dual sensitive microgel agent with size in the micrometer range. The microgel particle shrinks

© 2020 The Authors. Published by WILEY-VCH Verlag GmbH & Co. KGaA, Weinheim

when the temperature increases, whereby its volume phase transition temperature (VPTT) depends also on the pH value. Both parameters are adjusted to be in the physiological relevant window. The measured VPTT is around 38 °C at pH 5.0 and increases to 44 °C at pH 7.4. Composite membranes consisting of the new microgels, magnetic nanoparticles, and silk fibroin are prepared for controllable Rh.B release. The release is successfully triggered and controlled by changing the temperature and pH. It is found that with a higher temperature and more acidic pH, the release rate is increased as expected. Additionally, a higher content of microgel and smaller membrane thickness facilitate the release. Furthermore, we demonstrate the controlled release of Rh.B within 1 min triggered by the heating generated by magnetic nanoparticles via an alternating magnetic field of 16 mT at 111 kHz. With a higher absolute weight of magnetic nanoparticles, the release is increased due to the higher heating efficiency of MNPs. A control over two orders of magnitude of the release rate (0.01–5.0 μg min^{-1}) is achieved by tuning the content of microgels and magnetic nanoparticles, as well as the thickness of the membrane. A faster release rate is observed in acidic conditions with respect to the physiological value. The on-demand drug delivery system proposed in this work has unique characteristics that could make it suitable for future applications in the treatment of chronic diseases and tumors. Since silk fibroin is biodegradable in vivo due to the presence of enzymes,[24] the Rh.B release behavior may change. Consequently, more experiments related to degradation and system function lifetime should be performed before in vivo applications.

Experimental Section

Preparation of the Silk Fibroin Solution: The silk fibroin solution is prepared according to ref. [25]. The detailed procedures are described in the following. First, sericin is removed by boiling the silkworm cocoons in sodium carbonate (0.2 M) solution for 45 min. The obtained fibers are rinsed with deionized (DI) water and dried in a chemical hood overnight. Second, to further remove the impurities, the dried silk fibers are dissolved in lithium bromide (9.3 M) solution at 60 °C for 4 h. Afterward, the solution is purified by dialysis against DI water with Slide-A-Lyzer dialysis cassette (3500 MWCO, Thermo Scientific) for 2 days, followed by centrifugation at 4.4×10^3 rpm for 20 min twice, and finally by microfiltration with 5 μm filters twice. The purified silk fibroin solution is stored in the fridge before use.

Preparation of the Thermal and pH Sensitive Microgels (MGs): Thermal and pH sensitive hydrogel particles in micrometer scale size are synthesized by precipitation polymerization according to the ref. [17] with adjustments. Electrolyte methacrylic acid (MAA) with pKa around 5 is used in order to add pH sensitivity to the hydrogel particles. Meanwhile, isopropylmethacrylamide (NIPMAM) is used to shift the volume phase transition to a temperature higher than the physiological temperature (37 °C) since the methyl group of NIPMAM inhibits sterically the phase transition.[26] The feeding ratio of NIPAM/NIPMAM/MAA is 34/55/11. The detailed procedure is as below. First, N-isopropylacrylamide (NIPAM, 1002.5 mg), N-isopropylmethacrylamide (NIPMAM, 1817.5 mg), and methacrylic acid (MAA, 247.5 mg) are dissolved in DI water (375 mL), and then *N*, *N*-methylenebisacrylamide (MBA, 200 mg) is added inside as the cross-linker. The above solution is purged with nitrogen (N_2) for 30 min and then heated to 70 °C by an oil bath. Then the solution of ammonium persulfate (250 mg) dissolved in DI water (12.5 mL) is added to initiate the polymerization. The reaction proceeds for 5 h under N_2 at 70 °C. After cooling down, the suspension is purified with 14 kDa membrane by dialysis against DI water, and finally lyophilized to get dry microgels.

For the characterization, dynamic light scattering (DLS) is used to measure the diameter of the microgel in DI water. Then 0.1 M hydrochloric acid (HCl) and 0.1 M sodium hydroxide (NaOH) solution are used to adjust the pH of the microgel solution in water. In this paper, the phase transition temperature is defined as the temperature at which the microgel size is half of that of fully swollen and fully shrank state. The morphology of the microgel is observed by both scanning electron microscope (SEM) (GEMINI) and atomic force microscope (AFM) (Bruker). For the sample preparation, the solution of the microgel is drop cast on a silicon chip and then dried naturally. The dried sample is coated with 20 nm gold before SEM observation. Furthermore, its molecular structure is analyzed by Fourier-transform infrared spectroscopy (FTIR) (6700 Nicolet, Thermo Fischer Scientific) using the attenuated total reflection (ATR) mode. Each reported spectrum is the average of 32 scans collected at a resolution of 4 cm^{-1} in the wavenumber range of 650–4000 cm^{-1}. Then its thermal properties are characterized by thermogravimetric analysis (TGA) (TGA 4000, PerkinElmer) in the temperature range 30–850 °C at a heating rate of 20 °C min^{-1} under a nitrogen atmosphere.

Synthesis of the Magnetic Nanoparticles (MNPs): Magnetic nanoparticles are synthesized following an earlier described procedure.[10] The recipe is as follows. Under the nitrogen protection, iron(III) chloride ($FeCl_3$, 15.2 g) and iron(II) chloride tetrahydrate ($FeCl_2{\cdot}4H_2O$, 15.6 g) are dissolved in DI water (62.5 mL) in a three-neck flask, then ammonium hydroxide (28%, 32.5 mL) is added dropwise. After stirring for another 10 min, the solution of poly(ethylene oxide) (8 kDa) (PEO, 5 g) dissolved in DI water (50 mL) is added. Then the mixture is reacted at 70 °C for 2 h. Finally, the reacting solution is purified by magnetic separation against DI water (5 cycles) and concentrated to 10 mg mL^{-1}. To investigate the magnetic properties, the magnetization curve of the synthesized magnetic nanoparticles is measured by a superconducting quantum interference device (SQUID) (Quantum Design Magnetic Properties Measurement System).

Preparation and Characterization of Silk/MGs/MNPs Composite Membrane: The solution casting method is used to get the composite membrane by using the mixed solution of silk fibroin, microgels, and magnetic nanoparticles in a certain ratio. The detailed content of silk fibroin, MGs and MNPs used during preparation for each specific membrane is summarized in Table 1. After drying naturally in the ambient atmosphere, the composite membranes are obtained. In order to get water-stable membranes, the as-prepared membranes are immersed in 70% ethanol bath for 0.5 h and then dried again naturally in an ambient atmosphere to get the final membranes for the following experiments.

The cross-sectional morphologies of the above membranes are observed by the scanning electron microscope (GEMINI). For preparing membranes for SEM, the specimens are fractured in liquid nitrogen to avoid deformation, coated with iridium (5 nm), and attached to an aluminum plate by carbon tapes. Furthermore, to investigate the effect of ethanol annealing on the secondary structures and thermal-responsive properties of the composite membranes, FTIR and TGA characterization are carried out following the same procedure as for the microgels.

Relation between Rh.B Release Flux and Microgel Size: To find out how the release flux is related to the microgel size, the Rhodamine B (Rh.B) fluorescence dye is used as a model drug to study its release behavior. A hollow reservoir of $3.5 \times 3.5 \times 12$ mm^3 having a wall thickness of 1 mm is fabricated by a 3D printer (Formlabs) with commercial Clear Resin FLGPCL02. The reservoir is filled with Rh.B solution (100 μL, 100 mg mL^{-1}) in DI water. A piece of the composite membrane E (Silk/MGs/MNPs = 59/29/12) with an area of about 6×6 mm^2 is used to seal the reservoir with Scotch-Weld glue. The Rh.B solution filled reservoir is placed inside a 2 mL Eppendorf tube with acetate buffer (pH 5.0, 1.5 mL)/phosphate-buffered saline (PBS, pH 7.4, 1.5 mL). The Eppendorf tube is placed inside the oven at a given temperature (25, 30, 35, 40, 45, 50, and 55 °C). After 24 h, the fluorescence absorbance at 553 nm of the solution outside the reservoir

© 2020 The Authors. Published by WILEY-VCH Verlag GmbH & Co. KGaA, Weinheim

is measured by ultraviolet–visible spectroscopy (UV–vis) (Cary 100 Bio, Varian). Calibration curves for both acetate and PBS buffer are created for the conversion of absorbance values to Rh.B concentration (Figure S6, Supporting Information).

Thermally and pH Triggered Controllable Rhodamine B Release: In order to investigate how the microgel content and thickness influence the release kinetics of Rh.B, different composite membranes (A, B, E, F, G, and H) are used to seal the reservoir filled with Rh.B solution (100 µL, 100 mg mL^{-1}). Eppendorf tubes with acetate/PBS buffer solution (1.5 mL) is placed inside an oven at 25 and 45 °C independently. Then the reservoir is transferred to the Effendorf tube. After a certain time interval, the solution outside of the reservoir is replaced with the same fresh buffer (1.5 mL) and its fluorescence absorbance at 553 nm is measured by UV–vis spectroscopy.

Magnetically and pH Triggered Controllable Rhodamine B Release: To demonstrate the potential of using the Silk/MGs/MNPs composite membranes for controlled, magnetically triggered drug delivery applications, membranes (A, B, C, D, E, and F) with different contents of MGs and MNPs, and varying thicknesses are used to seal the reservoir filled with Rh.B solution (100 µL, 100 mg mL^{-1}). The reservoir is placed inside a glass vial (5 mL) with the composite membrane upside down to make sure that the Rh.B solution is in contact with the composite membrane. Acetate/PBS buffer solution (3 mL) is added to ensure that the position of the composite membrane is nearly in the central position of the solenoid coil after the glass vial is placed inside. An alternating magnetic field of 16 mT at 111 kHz is turned on and off for 3 times with each state lasting for 2 h during the experiment. A continuous flow set-up (Figure S9, Supporting Information) with two syringe pumps is built to provide a fresh buffer solution and also to monitor the real-time concentration of the solution outside the reservoir. The flow rate is set to be 0.05 mL min^{-1} for each syringe pump, the resulting inflow rate is 0.2 mL min^{-1}, and the outflow is collected every 5 min and its fluorescence absorbance at 553 nm is measured by UV–vis spectroscopy. The temperature of the solution outside the Rh.B containing reservoir is measured by the OSENSA's fiber optic temperature probe.

Supporting Information

Supporting Information is available from the Wiley Online Library or from the author.

Acknowledgements

This project is financially supported by the European Research Council (ERC) under the European Union's Horizon 2020 research and innovation program (Project "MEMS 4.0", ERC2016-ADG, Grant Agreement No. 742685), Microsystems Laboratory (LMIS1) lab funding from École Polytechnique Fédérale de Lausanne (EPFL), the China Scholarship Council (No. 201306270060), National Natural Science Foundation of China (No. 61804023), and Fundamental Research Funds for the Central Universities (No. ZYGX2019Z002).

Conflict of Interest

The authors declare no conflict of interest.

Keywords

magnetic field responsiveness, microgels, reversible drug delivery, smart membranes, tunable nano pores

Received: April 28, 2020
Revised: June 6, 2020
Published online:

[1] K. Park, *J. Controlled Release* **2014**, *190*, 3.
[2] Y. H. Yun, B. K. Lee, K. Park, *J. Controlled Release* **2015**, *219*, 2.
[3] S. Senapati, A. K. Mahanta, S. Kumar, P. Maiti, *Signal Transduction Targeted Ther.* **2018**, *3*, 7.
[4] A. Shademani, H. Zhang, J. K. Jackson, M. Chiao, *Adv. Funct. Mater.* **2017**, *27*, 1604558.
[5] D. J. Lim, H. Park, *J. Biomater. Sci., Polym. Ed.* **2018**, *29*, 750.
[6] P. Davoodi, L. Y. Lee, Q. Xu, V. Sunil, Y. Sun, S. Soh, C. H. Wang, *Adv. Drug Delivery Rev.* **2018**, *132*, 104.
[7] A. E. Deatsch, B. A. Evans, *J. Magn. Magn. Mater.* **2014**, *354*, 163.
[8] P. Zachkani, J. K. Jackson, F. N. Pirmoradi, M. Chiao, *RSC Adv.* **2015**, *5*, 98087.
[9] T. Hoare, J. Santamaria, G. F. Goya, S. Irusta, D. Lin, S. Lau, R. Padera, R. Langer, D. S. Kohane, *Nano Lett.* **2009**, *9*, 3651.
[10] T. Hoare, B. P. Timko, J. Santamaria, G. F. Goya, S. Irusta, S. Lau, C. F. Stefanescu, D. Lin, R. Langer, D. S. Kohane, *Nano Lett.* **2011**, *11*, 1395.
[11] Y. Guan, Y. Zhang, *Soft Matter* **2011**, *7*, 6375.
[12] S. Kim, K. Lee, C. Cha, *J. Biomater. Sci., Polym. Ed.* **2016**, *27*, 1698.
[13] S. Ashraf, H.-K. Park, H. Park, S.-H. Lee, *Macromol. Res.* **2016**, *24*, 297.
[14] Y. Chen, Y. Gao, L. P. da Silva, R. P. Pirraco, M. Ma, L. Yang, R. L. Reis, J. Chen, *Polym. Chem.* **2018**, *9*, 4063.
[15] M. Cao, Y. Wang, X. Hu, H. Gong, R. Li, H. Cox, J. Zhang, T. A. Waigh, H. Xu, J. R. Lu, *Biomacromolecules* **2019**, *20*, 3601.
[16] P. J. Dowding, B. Vincent, E. Williams, *J. Colloid Interface Sci.* **2000**, *221*, 268.
[17] H. Shimizu, R. Wada, M. Okabe, *Polym. J.* **2009**, *41*, 771.
[18] T. Still, K. Chen, A. M. Alsayed, K. B. Aptowicz, A. G. Yodh, *J. Colloid Interface Sci.* **2013**, *405*, 96.
[19] J. L. Wike-Hooley, J. Haveman, H. S. Reinhold, *Radiother. Oncol.* **1984**, *2*, 343.
[20] Y. Kato, S. Ozawa, C. Miyamoto, Y. Maehata, A. Suzuki, T. Maeda, Y. Baba, *Cancer Cell Int.* **2013**, *13*, 89.
[21] J. Liu, Y. Huang, A. Kumar, A. Tan, S. Jin, A. Mozhi, X. J. Liang, *Biotechnol. Adv.* **2014**, *32*, 693.
[22] A. Hervault, A. E. Dunn, M. Lim, C. Boyer, D. Mott, S. Maenosono, N. T. Thanh, *Nanoscale* **2016**, *8*, 12152.
[23] L. Liu, W. Yao, Y. Rao, X. Lu, J. Gao, *Drug Delivery* **2017**, *24*, 569.
[24] Q. Lu, B. Zhang, M. Li, B. Zuo, D. L. Kaplan, Y. Huang, H. Zhu, *Biomacromolecules* **2011**, *12*, 1080.
[25] D. N. Rockwood, R. C. Preda, T. Yucel, X. Wang, M. L. Lovett, D. L. Kaplan, *Nat. Protoc.* **2011**, *6*, 1612.
[26] M. Keerl, V. Smirnovas, R. Winter, W. Richtering, *Macromolecules* **2008**, *41*, 6830.

© 2020 The Authors. Published by WILEY-VCH Verlag GmbH & Co. KGaA, Weinheim